applied optics

Easily implemented approach for the calibration of alignment and retardation errors in a channeled spectropolarimeter

Xueping Ju,[1,2] Bin Yang,[3] Changxiang Yan,[1,*] Junqiang Zhang,[1,3] and Wenhe Xing[1,2]

[1]Changchun Institute of Optics, Fine Mechanics and Physics, Chinese Academy of Sciences, Changchun 130033, China
[2]China University of Chinese Academy of Sciences, Beijing 100049, China
[3]Yusense Information Technology and Equipment (Qingdao) Inc. Qingdao 266000, China
*Corresponding author: yancx0128@126.com

Received 24 July 2018; revised 11 September 2018; accepted 11 September 2018; posted 12 September 2018 (Doc. ID 340543); published 5 October 2018

Calibration of the channeled spectropolarimeter is significant for the quantitative application of this instrument. In current calibration methods for a channeled spectropolarimeter, an absolute angle between the coordinate system of an auxiliary polarizer and the global coordinate system of the instrument is usually indispensable. The effectiveness of calibration depends on the precision of the absolute angle, while it is usually difficult to achieve in a practical calibration process. This paper presents an easily implemented method to simultaneously calibrate the alignment and retardation errors of high-order retarders for a channeled spectropolarimeter. In the presented method, the requirement of an absolute angle between the coordinate system of an auxiliary polarizer and the global coordinate system of the instrument is replaced by only rotating a relative angle in the coordinate system of the auxiliary polarizer itself. First, we theoretically derive the modified reconstruction model considering the alignment errors of high-order retarders. By analyzing and summarizing the modified reconstruction model, the calibration and compensation models of the alignment and retardation errors are further proposed. Then, two linearly polarized beams with a relative angle of 45° between them are utilized to determine the alignment and retardation errors. Based on these results, the alignment and retardation errors can be compensated by a software correction algorithm without any precise mechanical adjustments. The effectiveness and feasibility of the presented method are verified by numerical simulations and experiments. The advantage of easy implementation makes this calibration method more suitable to apply in the laboratory and to be on track for correcting the channeled spectropolarimeter.

https://doi.org/10.1364/AO.57.008600

1. INTRODUCTION

Spectropolarimetry can measure the polarization parameters and spectral content of the light. It has been widely applied in various application fields, such as remote sensing [1,2], material characterization [3,4], and synthesis of novel materials [5,6]. Polarimetric spectral intensity modulation (PSIM), which was almost simultaneously proposed by Oka and Kato and Iannarilli *et al.* in 1999 [7,8], is a remarkable way for a channeled spectropolarimeter. Compared to traditional polarization and spectrum acquisition methods, it has several important advantages, such as the simplicity of the optical system, no mechanically movable components for polarization control or active devices for polarization modulation, and simultaneous measurement of spectrum and all Stokes parameters in snapshot mode [7].

Despite the advantages, application of the PSIM module also poses some problems. First, the alignment errors of two high-order retarders are inevitable. In theory, the orientations of a fast axis of two high-order retarders relative to the transmission of the polarizer are 0° and 45°, respectively. Owing to that polarization elements are directional, the nominal position of the fast axis of retarders is not totally consistent with the actual position. In addition, the assembly process of an instrument is not perfect; therefore, the alignment errors of high-order retarders are inevitable. The alignment errors can cause the changes of the reconstruction model, as will be shown in Section 3. Second, owing to the manufacture tolerance, the thicknesses of high-order retarders may deviate from the theoretical values. The variations of thickness of high-order retarders will cause the retardations to change, possibly introducing

calculation errors during the demodulation process of polarization parameters.

To solve the problems introduced by the fluctuation of retardations, Taniguchi *et al.* propose a reference beam calibration technique for calibrating the true phase factors used in the reconstruction process of polarization parameters [9]. Taniguchi *et al.* also put forward a self-calibration method to reduce the influences of fluctuation of high-order retarders' retardations for keeping the stability of the channeled spectropolarimeter [10]. However, it is noteworthy that the alignment errors of high-order retarders are ignored in both methods, weakening the reference beam calibration technique severely and even make the self-calibration method lose its advantages.

To solve the problems introduced by alignment errors, Mu *et al.* use two linearly polarized reference beams oriented at 22.5° and 45° (both angles are absolute angles) to calculate the orientation errors of two retarders [11]. While the effectiveness of this has been verified by simulations (without actual experiments), it has a critical drawback in that it works only when the orientation errors of two retarders are in different signs, thus restricting its application. Yang *et al.* propose a calibration method to determine the alignment errors and develop a correction algorithm to compensate for them [12]. While the alignment errors of retarders and a polarizer can be compensated for effectively, we must utilize an additional high-order retarder to determine the errors before the compensation process. Furthermore, the additional high-order retarder must be removed before the instrument works. The placement and removal of the additional high-order retarder increase the complexity of the system. We also propose a method to reduce the effects of alignment errors of high-order retarders using the amplitude items in the results of reference beam calibration technique [13]. In these methods, the alignment errors may be calibrated and well compensated for; however, the phase factors utilized in the reconstruction process are acquired by employing a reference beam, linearly polarized at 22.5°. This is an absolute angle between the coordinate system of the auxiliary polarizer and the global coordinate system of the instrument. The absolute angle is hard to achieve in a practical calibration process. On the other hand, it is found that the reconstructed polarization parameters are very sensitive to the precision of the orientation angle of the reference beam that is used for removing the phase factors [11].

In this paper, to overcome the drawback of requirement of an absolute angle, we put forward a new calibration method, which employs two linearly polarized beams whose crossing angle is relatively 45°. The whole calibration process can be divided into two procedures. In the first step, we use a linearly polarized beam whose polarization orientation is arbitrary to illuminate the channeled spectropolarimeter and record the measurement results. In the second step, we use the other linearly polarized beam whose polarization orientation is 45° relative to the first (rotate the auxiliary polarizer based on its initial state) to illuminate the instrument and also record the measurement results. Using the measurement results of two calibration procedures, we can simultaneously calibrate the alignment and retardation errors of high-order retarders. In short, the calibration condition is merely putting an auxiliary polarizer in front of the PSIM module and rotating it by 45°. In the aspect of operation for achieving the angle's requirement in practice, rotating a relative angle based on the coordinate system of the auxiliary polarizer is easier to implement than achieving an absolute angle between two different coordinate systems. (One is the own coordinate system of the auxiliary polarizer, and the other is the global coordinate system of the instrument.) The advantage of easy implementation makes the presented method more for practical applications. We theoretically analyze the modified reconstruction model and derive the calibration and compensation models of the alignment and retardation errors. Based on the calibration and compensation models, it is obvious that the orientation of the first linearly polarized beam does not affect the effectiveness of the presented method, which will be shown in Section 3.A. We merely need to make sure the orientation of the second linearly polarized beam is 45° relative to the first, which is easy to achieve using an encoder. The effectiveness of the proposed method is verified by numerical simulations. The results show that utilizing the presented method, the measurement accuracy of polarization parameters can be improved by at least one order of magnitude. The validity of this method is further verified by experiments.

This paper is structured as follows. In Section 2, we first review the principle of a channeled spectropolarimeter, and then based on the theoretical reconstruction model, we illustrate the influences of polarization orientation errors of the reference beam on the accuracy of the channeled spectropolarimeter by numerical simulations. In Section 3, based on the modified reconstruction model, we theoretically derive the calibration and compensation model of the alignment and retardation errors of high-order retarders and put forward a method to simultaneously calibrate the polarization errors of high-order retarders. Section 4 verifies the effectiveness and feasibility of this proposed method by numerical simulations. Section 5 further validates the proposed method by experimental tests, and conclusions are presented in Section 6.

2. INFLUENCES INTRODUCED BY THE POLARIZATION ORIENTATION ERROR OF THE SPECIFIC REFERENCE BEAM ON THE CLASSIC CALIBRATION METHOD OF A CHANNELED SPECTROPOLARIMETER

In this section, we briefly review the theoretical polarization measurement process of a channeled spectropolarimeter. Based on the theoretical reconstruction model, we simulate the measurement process in the presence of different polarization orientation errors of the specific reference beam. Simulation results apparently show that the reconstruction accuracy of polarization parameters is very sensitive to the polarization orientation errors of the reference beam.

A. Review of the Principle of a Channeled Spectropolarimeter

Channeled spectropolarimetry is a technique that converses a spectrometer into a spectropolarimeter through the simple addition of the PSIM module to the optical system. The optical schematic of a spectrometer and PSIM module is shown in Fig. 1. The PSIM module consists of two high-order retarders,

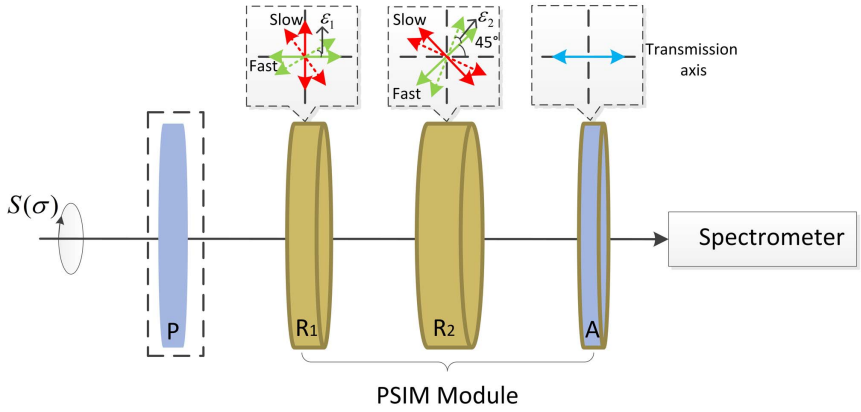

Fig. 1. Sketch of a channeled spectropolarimeter and the alignment errors of R_1 and R_2.

R_1 and R_2 with thicknesses d_1 and d_2, and the polarizer, A. The polarizer P in the dashed box is merely utilized to generate the target light and reference beams during the calibration process.

In this paper, all angles mentioned are with reference to the transmission axis of polarizer A illustrated in Fig. 1. In theory, as shown in Fig. 1, the transmission axis of polarizer A is horizontal, and the fast axes of R_1 and R_2 are 0° and 45°, respectively. In fact, however, due to the alignment errors, the orientation errors of fast axes of R_1 and R_2 are unavoidable. ε_1 and ε_2 are the alignment errors of R_1 and R_2, respectively, as depicted in Fig. 1, which will be utilized in Section 3.

The polarization parameters of a light passing through a channeled spectropolarimeter can be most conveniently represented in terms of the Stokes vector representation $S = [S_0 S_1 S_2 S_3]^T$. The Stokes vector of a target light launched into the spectrometer is expressed

$$S_{\text{out}}(\sigma) = M_A(0°) \cdot M_{R_2}\{45°, \varphi_2(\sigma)\} \cdot M_{R_1}\{0°, \varphi_1(\sigma)\} \cdot S_{\text{in}}(\sigma), \tag{1}$$

where $S_{\text{in}}(\sigma)$ and $S_{\text{out}}(\sigma)$ denote the Stokes vectors of incident and transmitted target light, respectively, and σ is the wavenumber. M_{R_1}, M_{R_2}, and M_A stand for the Mueller matrices of R_1, R_2, and A, respectively. $\varphi_j(\sigma)(j = 1, 2)$ is the phase retardation of R_1 and R_2. The spectrum obtained by the spectrometer is expressed as [7]

$$\begin{aligned} B(\sigma) = {} & \frac{1}{2}S_0(\sigma) \\ & + \frac{1}{8}S_{23}^*(\sigma)\exp[-i\{\varphi_2(\sigma) - \varphi_1(\sigma)\}] \\ & + \frac{1}{8}S_{23}(\sigma)\exp[i\{\varphi_2(\sigma) - \varphi_1(\sigma)\}] \\ & + \frac{1}{4}S_1(\sigma)\exp[-i\varphi_2(\sigma)] \\ & + \frac{1}{4}S_1(\sigma)\exp[i\varphi_2(\sigma)] \\ & - \frac{1}{8}S_{23}(\sigma)\exp[-i\{\varphi_1(\sigma) + \varphi_2(\sigma)\}] \\ & - \frac{1}{8}S_{23}^*(\sigma)\exp[i\{\varphi_1(\sigma) + \varphi_2(\sigma)\}], \end{aligned} \tag{2}$$

where $S_{23}(\sigma) = S_2(\sigma) + iS_3(\sigma)$, and $S_{23}^*(\sigma)$ is the conjugate of $S_{23}(\sigma)$. $S_k(\sigma)(k = 0\ldots3)$ denotes the Stokes parameters contained in $S_{\text{in}}(\sigma)$. Computing the autocorrelation function of $B(\sigma)$ with the inverse Fourier transformation, Stokes parameters are modulated to several different frequency domain regions, which are called "channels." The channels distributing in frequency domain are given by

$$\begin{aligned} C(h) = {} & C_0(h) + C_1[h - (L_1 - L_2)] + C_1^*[-h - (L_1 - L_2)] \\ & + C_2(h - L_2) + C_2^*(-h - L_2) + C_3[h - (L_1 + L_2)] \\ & + C_3^*[-h - (L_1 + L_2)], \end{aligned} \tag{3}$$

where

$$C_0(h) = \mathcal{F}^{-1}\left\{\frac{1}{2}S_0(\sigma)\right\}, \tag{4}$$

$$C_2(h) = \mathcal{F}^{-1}\left\{\frac{1}{4}S_1(\sigma)\exp[-i\varphi_2(\sigma)]\right\}, \tag{5}$$

$$C_3(h) = \mathcal{F}^{-1}\left\{-\frac{1}{8}S_{23}(\sigma)\exp[-i(\varphi_1(\sigma) + \varphi_2(\sigma))]\right\}, \tag{6}$$

and h is the variable in frequency domain conjugate to σ under the Fourier transformation. $L_p(p = 1, 2)$ stands for the actual optical path difference introduced by R_1 and R_2 in the central wavenumber [14]. The desired channels, C_0, C_2, and C_3 centered at $h = 0$, $h = L_2$, and $h = L_1 + L_2$, respectively, are then filtered out by the frequency filtering technique independently, and Fourier transformations are then performed. The results are expressed as

$$\mathcal{F}\{C_0(h)\} = \frac{1}{2}S_0(\sigma), \tag{7}$$

$$\mathcal{F}\{C_2(h)\} = \frac{1}{4}S_1(\sigma)\exp[-i\varphi_2(\sigma)], \tag{8}$$

$$\mathcal{F}\{C_3(h)\} = -\frac{1}{8}S_{23}(\sigma)\exp[-i(\varphi_1(\sigma) + \varphi_2(\sigma))]. \tag{9}$$

As mentioned before, $\varphi_1(\sigma)$ and $\varphi_2(\sigma)$ are the phase retardations of R_1 and R_2, which are merely the function of parameters of retarders and wavenumber. To calibrate the phase factors, $\exp[i\varphi_2(\sigma)]$ and $\exp[i(\varphi_1(\sigma) + \varphi_2(\sigma))]$, a reference beam

linearly polarized oriented at 22.5° is employed [9,10]. It is a very representative method in that its principle is widely utilized in other methods to calibrate the phase factors. Stokes parameters of the reference beam passing through the PSIM module are given by

$$S_1(\sigma) = \frac{\sqrt{2}}{2} S_0(\sigma), \tag{10}$$

$$S_2(\sigma) = \frac{\sqrt{2}}{2} S_0(\sigma), \tag{11}$$

$$S_3(\sigma) = 0. \tag{12}$$

Combining [Eqs. (7)–(9)] and [Eqs. (10)–(12)], the phase factors are given by

$$\exp[-i\varphi_2(\sigma)] = 2\sqrt{2}\frac{\mathcal{F}\{C_{2,22.5^\circ}(h)\}}{\mathcal{F}\{C_{0,22.5^\circ}(h)\}}, \tag{13}$$

$$\exp[-i(\varphi_1(\sigma) + \varphi_2(\sigma))] = -4\sqrt{2}\frac{\mathcal{F}\{C_{3,22.5^\circ}(h)\}}{\mathcal{F}\{C_{0,22.5^\circ}(h)\}}. \tag{14}$$

After eliminating the phase factors, the whole Stokes parameters of the incident target light have been acquired as

$$S_0(\sigma) = 2|\mathcal{F}\{C_0(h)\}|, \tag{15}$$

$$S_1(\sigma) = \left|\sqrt{2}\frac{\mathcal{F}\{C_2(h)\} \cdot \mathcal{F}\{C_{0,22.5^\circ}(h)\}}{\mathcal{F}\{C_{2,22.5^\circ}(h)\}}\right|, \tag{16}$$

$$S_2(\sigma) = \mathrm{Re}\left[\frac{\sqrt{2}}{2}\frac{\mathcal{F}\{C_3(h)\} \cdot \mathcal{F}\{C_{0,22.5^\circ}(h)\}}{\mathcal{F}\{C_{3,22.5^\circ}(h)\}}\right], \tag{17}$$

$$S_3(\sigma) = \mathrm{Im}\left[\frac{\sqrt{2}}{2}\frac{\mathcal{F}\{C_3(h)\} \cdot \mathcal{F}\{C_{0,22.5^\circ}(h)\}}{\mathcal{F}\{C_{3,22.5^\circ}(h)\}}\right], \tag{18}$$

where Re is the operator to extract the real part, and Im is the operator to extract the imaginary part.

B. Effects of Polarization Orientation Error of the Specific Linearly Polarized Beam on the Reference Beam Calibration Technique

The reference beam calibration technique introduced in Ref. 9 has provided a classic principle to calibrate the phase factors. It is noteworthy that the reference beam calibration technique utilizes a reference beam with ideal polarization orientation (22.5°). As mentioned in Section 1, it is a requirement of the absolute angle between the own coordinate system of the auxiliary polarizer and the global coordinate of the instrument, something that is difficult to achieve in a practical calibration process. On the other hand, the reconstructed polarization parameters are very sensitive to the orientation angle of the reference beam that is used in all previous methods for removing the phase factors [11]. In this paper, to clearly show the influences of polarization orientation error on the reference beam calibration technique, we first theoretically derive the modified calibration model when the polarization orientation of the reference beam deviates from 22.5° and then simulate the demodulation process using different phase factors obtained by the reference beam calibration technique in the presence of different polarization orientation errors.

When the polarization orientation error exists, Stokes parameters of the reference beam shown in [Eqs. (10) and (11)] will be changed to

$$S_{1,22.5+\eta}(\sigma) = \frac{\sqrt{2}}{2}(\cos 2\eta - \sin 2\eta) S_0(\sigma), \tag{19}$$

$$S_{2,22.5+\eta}(\sigma) = \frac{\sqrt{2}}{2}(\cos 2\eta + \sin 2\eta) S_0(\sigma), \tag{20}$$

where η is the polarization orientation error of the reference beam. Consequently, the calibration results of phase factors shown in [Eqs. (13) and (14)] also change. These are given by

$$\exp[-i\varphi_2(\sigma)]_{22.5+\eta} = \frac{2\sqrt{2}}{\cos 2\eta - \sin 2\eta}\frac{\mathcal{F}\{C_{2,22.5^\circ+\eta}(h)\}}{\mathcal{F}\{C_{0,22.5^\circ+\eta}(h)\}}, \tag{21}$$

$$\exp[-i(\varphi_1(\sigma) + \varphi_2(\sigma))]_{22.5+\eta} = \frac{-4\sqrt{2}}{\cos 2\eta + \sin 2\eta}\frac{\mathcal{F}\{C_{3,22.5^\circ+\eta}(h)\}}{\mathcal{F}\{C_{0,22.5^\circ+\eta}(h)\}}. \tag{22}$$

As shown in [Eqs. (21) and (22)], because the amplitude items of the phase factors vary with the polarization orientation error, the effectiveness of the reference beam calibration technique will be weakened. Next, we utilize the numerical simulation to intuitively express the influences of the polarization orientation error. In the simulations, the Stokes parameters to be measured are set as $S_1 = S_2 = S_3 = \sqrt{3}/3S_0$. The wavenumber range is 14, 954–18, 408 cm^{-1}, and the thicknesses of R_1 and R_2 are 3.0 mm and 6.0 mm, respectively. The high-order retarders are made of quartz, whose birefringence in the selected waveband can be consulted in Ref. [15]. The influences of the polarization orientation error on the reference beam calibration technique are shown in Fig. 2. It is necessary to explain that the fluctuation of reconstruction results may be caused by the ringing in the channeled spectropolarimeter reconstruction, but we have alleviated the influences by introducing apodization using the Hann window [16]. As shown in Table 1, the data in the first line demonstrate that the calculation errors (with the order of 10^{-6} or 10^{-7}) will not affect the conclusions (with the order of 10^{-2} or 10^{-3}) in the following discussions. To be consistent with the specifications used in Refs. [17–19], the degree of polarization (DoP) utilized in this paper is calculated by the first three Stokes parameters; it is, strictly speaking, the degree of linear polarization (DoLP).

As shown in Fig. 2 and Table 1, the reconstruction errors of polarization parameters grow larger as the polarization orientation error of the reference beam increases. Those influences of the polarization orientation error on the accuracy of polarization measurement cannot be ignored during the calibration of a channeled spectropolarimeter. To satisfy the requirements of actual applications, the designed goal of uncertainty of DoP measurement is 0.002–0.005, which varies with the DoP of a target light [17–19]. The expressions are given by

$$\begin{cases} 0.002, (\mathrm{DoP} < 0.2) \\ 0.002 + 0.375(\mathrm{DoP} - 0.2), (0.2 \le \mathrm{DoP} \le 1) \end{cases}. \tag{23}$$

It is worth noting that the specification is the total measurement uncertainty of DoP for the channeled spectropolarimeter, meaning that the acceptable measurement uncertainty of

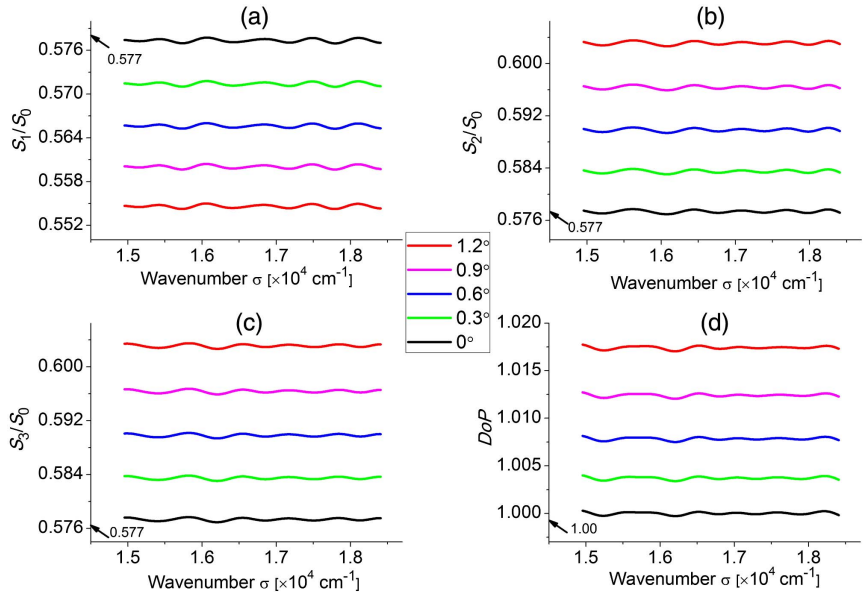

Fig. 2. Reconstruction results of polarization parameters when the reference beam has different polarization orientation errors. The reference values are $S_1/S_0 = S_2/S_0 = S_3/S_0 = 0.577$, DoP = 1.00.

DoP introduced by the polarization orientation error is much smaller. For instance, when the assigned measurement uncertainties of DoP introduced by the polarization orientation error is 50% of the total measurement uncertainties of DoP, i.e., the DoP measurement error is less than 0.002 for the target light whose DoP is 0.75, according to Table 1, the polarization orientation error must be limited to less than 0.3°. The requirements of the polarization orientation error are relatively small in a practical calibration process of the channeled spectropolarimeter. Therefore, it is not encouraged to use fine mechanical adjustments during the assembly and calibration to keep the precision of the polarization orientation of the reference beam.

It is noteworthy to explain that, to the best of our knowledge, the uncertainty of DoP measurement has not been achieved to 0.002–0.005 using the PSIM technique in practical applications. To improve the precision of a channeled spectropolarimeter, on the one hand, we can reduce the impact of the detecting principle defect, which is called "crosstalk" across the desired channels C_0, C_2, and C_3 [20]. Recently, Zhang *et al.* put forward a full Stokes imaging spectropolarimeter, whose significant advantages are that the errors in the reconstructed polarization parameters caused by aliasing between desired channels are suppressed effectively; meanwhile, the reconstructed spectra retain the resolution of the interference spectrometer [20]. Quan *et al.* propose a channeled polarimetric technique to measure the linear Stokes parameters [21,22]. It also has the advantages of improving the resolution of the reconstructed spectrum and reducing the effects of crosstalk between desired channels. This research has significant importance to overcome the detecting principle defect of the channeled spectropolarimetry. On the other hand, the calibration and compensation of systematic errors of the essential polarization components (such as two high-order retarders) are an effective way to further improve the precision of a channeled spectropolarimeter.

To address the limitation of a strict requirement of the absolute angle, we propose a new calibration method using two linearly polarized reference beams with a relative angle of 45° between them. The polarization orientation of the first reference beam is arbitrary, and we just keep the polarization orientation of the second reference beam of 45° relative to the first. It is easier to implement in a practical calibration. Utilizing the presented method can simultaneously calibrate the alignment errors and the actual retardations of two high-order retarders, meaning that the presented method is more suitable for application to the calibration of a channeled spectropolarimeter.

Table 1. Reconstruction Errors of Polarization Parameters Introduced by Different Polarization Orientation Errors of the Reference Beam

Situation	S1/S0 Error	S2/S0 Error	S3/S0 Error	DoP Error
0 deg	9.97×10^{-7}	4.33×10^{-6}	-3.16×10^{-6}	1.31×10^{-6}
0.3 deg	-5.95×10^{-3}	6.15×10^{-3}	6.14×10^{-3}	3.71×10^{-3}
0.6 deg	-1.17×10^{-2}	1.25×10^{-2}	1.25×10^{-2}	7.84×10^{-3}
0.9 deg	-1.73×10^{-2}	1.90×10^{-2}	1.90×10^{-2}	1.24×10^{-2}
1.2 deg	-2.27×10^{-2}	2.58×10^{-2}	2.58×10^{-2}	1.74×10^{-2}

3. CALIBRATION AND COMPENSATION OF THE ALIGNMENT AND RETARDATION ERRORS OF TWO HIGH-ORDER RETARDERS

In this section, we analyze and summarize the modified reconstruction model of the channeled spectropolarimeter that takes the alignment errors of R_1 and R_2 into consideration. Based on the modified reconstruction model, we theoretically derive the calibration and compensation models of the alignment and retardation errors of two high-order retarders. An easily implemented approach using two linearly polarized

beams with a relative angle of 45° between them for calibrating and compensating the alignment and retardation errors of two high-order retarders is proposed. It is effective to reduce the effects of alignment and retardation errors of high-order retarders for the channeled spectropolarimeter.

A. Derivation of the Calibration Models

Because the alignment errors of high-order retarders are inevitable, we first calculate the Stokes vector of the transmitted light considering the effects of alignment errors. This is expressed as

$$S_{\text{out}}'(\sigma) = M_A(0°) \cdot M_{R_2}\{45° + \varepsilon_2, \varphi_2(\sigma))\} \cdot M_{R_1}\{\varepsilon_1, \varphi_1(\sigma)\} \cdot S_{\text{in}}(\sigma), \tag{24}$$

where $S_{\text{out}}'(\sigma)$ denotes the Stokes vector of the transmitted target light in the presence of the alignment errors. ε_1 and ε_2 are the alignment errors of R_1 and R_2, respectively, as depicted in Fig. 1. Based on the principle used in Section 2, the modulated spectrum obtained by the spectrometer can be given by

$$\begin{aligned} B'(\sigma) = {} & \frac{1}{2}\{S_0(\sigma) + ce \cdot \{b \cdot S_1(\sigma) + a \cdot S_2(\sigma)\}\} \\ & - \frac{1}{8}d(1+e)\{a \cdot S_1(\sigma) - b \cdot S_2 \\ & + iS_3(\sigma)\} \exp[-i\{\varphi_2(\sigma) - \varphi_1(\sigma)\}] \\ & - \frac{1}{8}d(1+e)\{a \cdot S_1(\sigma) - b \cdot S_2 \\ & - iS_3(\sigma)\} \exp[i\{\varphi_2(\sigma) - \varphi_1(\sigma)\}] \\ & + \frac{1}{4}df\{b \cdot S_1(\sigma) + a \cdot S_2(\sigma)\} \exp[-i\varphi_2(\sigma)] \\ & + \frac{1}{4}df\{b \cdot S_1(\sigma) + a \cdot S_2(\sigma)\} \exp[i\varphi_2(\sigma)] \\ & + \frac{1}{8}d(1-e)\{a \cdot S_1(\sigma) - b \cdot S_2(\sigma) \\ & - iS_3(\sigma)\} \exp[-i\{\varphi_1(\sigma) + \varphi_2(\sigma)\}] \\ & + \frac{1}{8}d(1-e)\{a \cdot S_1(\sigma) - b \cdot S_2(\sigma) \\ & + iS_3(\sigma)\} \exp[i\{\varphi_1(\sigma) + \varphi_2(\sigma)\}] \\ & + \frac{1}{4}cf\{a \cdot S_1(\sigma) - b \cdot S_2(\sigma) - iS_3(\sigma)\} \exp[-i\varphi_1(\sigma)] \\ & + \frac{1}{4}cf\{a \cdot S_1(\sigma) - b \cdot S_2(\sigma) + iS_3(\sigma)\} \exp[i\varphi_1(\sigma)], \end{aligned} \tag{25}$$

where $a = \sin(2\varepsilon_1)$, $b = \cos(2\varepsilon_1)$, $c = \sin(2\varepsilon_2)$, $d = \cos(2\varepsilon_2)$, $e = \sin\{2(\varepsilon_2 - \varepsilon_1)\}$, and $f = \cos\{2(\varepsilon_2 - \varepsilon_1)\}$. Comparing [Eq. (2)] and [Eq. (25)], owing to the existence of alignment errors of high-order retarders, the contents contained in desired channels C_0 C_2 and C_3 are the mixing of different Stokes parameters. Besides, two new channels C_4 and C_4^* centered at $h = L_1$ and $h = -L_1$, respectively, have been created. Because of the thickness ratio of R_1 and R_2 being 1:2, the channels C_4 and C_4^* are almost overlapped with C_1 and C_1^*, causing the channeled spectropolarimeter to lose the potential of self-calibration utilized in Ref. [10].

Because the alignment errors of high-order retarders are relatively small, the second-order and high-order small quantities contained in channel C_0, i.e., the coefficients *ceb* and *cea* in [Eq. (25)], have been ignored. Computing the autocorrelation function of $B'(\sigma)$ with the inverse Fourier transformation, the result is expressed as

$$\begin{aligned} C'(h) = {} & C_0'(h) + C_1'[h - (L_1 - L_2)] + C_1'^*[-h - (L_1 - L_2)] \\ & + C_2'(h - L_2) + C_2'^*(-h - L_2) + C_3'[h - (L_1 + L_2)] \\ & + C_3'^*[-h - (L_1 + L_2)] + C_4'(h - L_1) + C_4'^*(-h - L_1), \end{aligned} \tag{26}$$

where

$$C_0'(h) = \mathcal{F}^{-1}\left\{\frac{1}{2}S_0(\sigma)\right\}, \tag{27}$$

$$C_2'(h) = \mathcal{F}^{-1}\left\{\frac{1}{4}df\{b \cdot S_1(\sigma) + a \cdot S_2(\sigma)\} \exp[-i\varphi_2(\sigma)]\right\}, \tag{28}$$

$$\begin{aligned} C_3'(h) = \mathcal{F}^{-1}\Big\{ & \frac{1}{8}d(1-e)\{a \cdot S_1(\sigma) - b \cdot S_2(\sigma) \\ & - iS_3(\sigma)\} \exp[-i\{\varphi_1(\sigma) + \varphi_2(\sigma)\}]\Big\}. \end{aligned} \tag{29}$$

Comparing Eqs. (4)–(6) to Eqs. (27)–(29), the reconstruction model has been changed by the alignment errors apparently. The Stokes parameters directly reconstructed from desired channels $C_2'(h)$ and $C_3'(h)$ are not the true values because of the influences of the alignment errors of high-order retarders. Considering that the alignment errors are relatively small, fine mechanical adjustments will be costly. Furthermore, it is inconvenient to adjust when the channeled spectropolarimeter is in orbit. Therefore, we must employ an easily implemented calibration method to reduce the influences of the alignment and retardation errors of high-order retarders after assembly for keeping the accuracy of a channeled spectropolarimeter. Based on the results of derivation, we put forward a new approach to simultaneously calibrate the alignment and retardation errors of high-order retarders using two linearly polarized beams with a relative angle of 45°.

For a linearly polarized light, oriented at an arbitrary angle θ, its Stokes vector can be expressed as

$$S_{\text{LP},\theta}(\sigma) = S_0^\theta(\sigma) \cdot [1 \ \cos(2\theta) \ \sin(2\theta) \ 0]^T, \tag{30}$$

where $S_{\text{LP},\theta}(\sigma)$ denotes the Stokes vector, and $S_0^\theta(\sigma)$ denotes the first parameter in the Stokes vector. When it passes through the channeled spectropolarimeter with alignment errors, the contents in the desired channels are expressed as

$$\mathcal{F}(C_{0,\theta}) = \frac{1}{2}S_0(\sigma), \tag{31}$$

$$\mathcal{F}(C_{2,\theta}) = \frac{1}{4}df\{b \cdot S_1(\sigma) + a \cdot S_2(\sigma)\} \exp[-i\varphi_2(\sigma)], \tag{32}$$

$$\begin{aligned} \mathcal{F}(C_{3,\theta}) = {} & \frac{1}{8}d(1-e)\{a \cdot S_1(\sigma) - b \cdot S_2(\sigma) \\ & - iS_3(\sigma)\} \exp[-i\{\varphi_1(\sigma) + \varphi_2(\sigma)\}]. \end{aligned} \tag{33}$$

Combining Eq. (30) with Eqs. (31)–(33), we can get the expressions as

$$\frac{\mathcal{F}(C_{2,\theta})}{\mathcal{F}(C_{0,\theta})}=\frac{1}{2}df(b\cdot\cos 2\theta+a\cdot\sin 2\theta)\cdot\exp[-i\varphi_2(\sigma)], \tag{34}$$

$$\frac{\mathcal{F}(C_{3,\theta})}{\mathcal{F}(C_{0,\theta})}=\frac{1}{4}d\{1-e\}\cdot(a\cdot\cos 2\theta-b\cdot\sin 2\theta)\cdot\exp[-i\{\varphi_1(\sigma)+\varphi_2(\sigma)\}]. \tag{35}$$

When the polarizer P rotates a relative angle α with respect to its initial state, Eqs. (34) and (35) will change to

$$\frac{\mathcal{F}(C_{2,\theta+\alpha})}{\mathcal{F}(C_{0,\theta+\alpha})}=\frac{1}{2}df\{b\cdot\cos 2(\theta+\alpha)+a\cdot\sin 2(\theta+\alpha)\}\cdot\exp[-i\varphi_2(\sigma)], \tag{36}$$

$$\frac{\mathcal{F}(C_{3,\theta+\alpha})}{\mathcal{F}(C_{0,\theta+\alpha})}=\frac{1}{4}d\{1-e\}\{a\cdot\cos 2(\theta+\alpha)-b\cdot\sin 2(\theta+\alpha)\}\cdot\exp[-i\{\varphi_1(\sigma)+\varphi_2(\sigma)\}]. \tag{37}$$

Combining Eqs. (34) and (35) with Eq. (36), we can calculate and obtain the equations as

$$\frac{\mathrm{abs}\left[\frac{\mathcal{F}(C_{2,\theta+\alpha})}{\mathcal{F}(C_{0,\theta+\alpha})}\right]}{\mathrm{abs}\left[\frac{\mathcal{F}(C_{3,\theta})}{\mathcal{F}(C_{0,\theta})}\right]}=2\cdot\frac{f}{1-e}\left|\frac{b\cdot\cos 2(\theta+\alpha)+a\cdot\sin 2(\theta+\alpha)}{a\cdot\cos 2\theta_1-b\cdot\sin 2\theta}\right|, \tag{38}$$

$$\left\{2\cdot\frac{\mathrm{abs}\left[\frac{\mathcal{F}(C_{2,\theta})}{\mathcal{F}(C_{0,\theta})}\right]}{f}\right\}^2+\left\{4\cdot\frac{\mathrm{abs}\left[\frac{\mathcal{F}(C_{3,\theta})}{\mathcal{F}(C_{0,\theta})}\right]}{1-e}\right\}^2=\cos^2(2\varepsilon_2), \tag{39}$$

where abs stands for the operation of taking the absolute value.

By analyzing Eqs. (38) and (39), we can find that the alignment errors of high-order retarders can be figured out by selecting a suitable α to eliminate the variable θ. That is to say, the suitable α should satisfy the following conditions:

$$\begin{cases}\cos 2(\theta+\alpha)=-\sin 2\theta\\ \sin 2(\theta+\alpha)=\cos 2\theta\end{cases},\quad\text{or}\quad\begin{cases}\cos 2(\theta+\alpha)=\sin 2\theta\\ \sin 2(\theta+\alpha)=-\cos 2\theta\end{cases}. \tag{40}$$

Considering the limiting condition of $|2\alpha|\le\pi$, we can conclude that $\alpha=\pi/4$ or $\alpha=-\pi/4$. That is to say, two linearly polarized beams used in the presented method are generated by putting the polarizer P depicted in Fig. 1 in an arbitrary orientation and then rotated by 45° in an arbitrary direction. To achieve the best modulation results of both channels C_2 and C_3, the ideal orientation of the first linearly polarized beam is close to 22.5°, and it is necessary to emphasize that the exact position does not need to be known.

Next, we take the example $\alpha=\pi/4$ to demonstrate the calibration process. For the condition of $\alpha=\pi/4$, Eqs. (36)–(38) change to

$$\frac{\mathcal{F}(C_{2,\theta+\alpha})}{\mathcal{F}(C_{0,\theta+\alpha})}=\frac{1}{2}df\{-b\cdot\sin 2\theta+a\cdot\cos 2\theta\}\cdot\exp[-i\varphi_2(\sigma)], \tag{41}$$

$$\frac{\mathcal{F}(C_{3,\theta+\alpha})}{\mathcal{F}(C_{0,\theta+\alpha})}=\frac{1}{4}d\{1-e\}\{-a\cdot\sin 2\theta-b\cdot\cos 2\theta\}\cdot\exp[-i\{\varphi_1(\sigma)+\varphi_2(\sigma)\}], \tag{42}$$

$$\frac{\mathrm{abs}\left[\frac{\mathcal{F}(C_{2,\theta+\alpha})}{\mathcal{F}(C_{0,\theta+\alpha})}\right]}{\mathrm{abs}\left[\frac{\mathcal{F}(C_{3,\theta})}{\mathcal{F}(C_{0,\theta})}\right]}=2\cdot\frac{f}{1-e}. \tag{43}$$

Because the alignment errors of high-order retarders ε_1 and ε_2 are small quantities, the parameters $1-e$ and f are approximately equal to 1. (They are denominators; therefore, they cannot equal zero.) The sign of the coefficients of each term in Eqs. (32) and (33) also can be determined, such as $d>0$, $f>0$, and $1-e>0$. We assume that $\varepsilon_2>0$, which is dependent on the manufacturing tolerances of the channeled spectropolarimeter. Combing Eqs. (39) and (43), the alignment errors of high-order retarders ε_1 and ε_2 can be determined. They are given by

$$\varepsilon_1=\frac{\arccos\left(\sqrt{B}\right)-\arccos\left(\frac{A^2-1}{A^2+1}\right)}{2}, \tag{44}$$

$$\varepsilon_2=\frac{\arccos\left(\sqrt{B}\right)}{2}, \tag{45}$$

where

$$A=\frac{\mathrm{abs}\left[\frac{\mathcal{F}(C_{2,\theta+\alpha})}{\mathcal{F}(C_{0,\theta+\alpha})}\right]}{\mathrm{abs}\left[\frac{\mathcal{F}(C_{3,\theta})}{\mathcal{F}(C_{0,\theta})}\right]}, \tag{46}$$

$$B=\left\{2\cdot\frac{\mathrm{abs}\left[\frac{\mathcal{F}(C_{2,\theta})}{\mathcal{F}(C_{0,\theta})}\right]}{f}\right\}^2+\left\{4\cdot\frac{\mathrm{abs}\left[\frac{\mathcal{F}(C_{3,\theta})}{\mathcal{F}(C_{0,\theta})}\right]}{1-e}\right\}^2. \tag{47}$$

Combining Eqs. (34) and (35) with Eqs. (41) and (42), we can calculate that

$$\left\{\frac{\mathcal{F}(C_{2,\theta})}{\mathcal{F}(C_{0,\theta})}\right\}^2+\left\{\frac{\mathcal{F}(C_{2,\theta+\alpha})}{\mathcal{F}(C_{0,\theta+\alpha})}\right\}^2=\frac{1}{4}d^2f^2\cdot\exp[-i2\varphi_2(\sigma)], \tag{48}$$

$$\left\{\frac{\mathcal{F}(C_{3,\theta})}{\mathcal{F}(C_{0,\theta})}\right\}^2+\left\{\frac{\mathcal{F}(C_{3,\theta+\alpha})}{\mathcal{F}(C_{0,\theta+\alpha})}\right\}^2=\frac{1}{16}d^2(1-e)^2\cdot\exp[-i2\{\varphi_1(\sigma)+\varphi_2(\sigma)\}]. \tag{49}$$

As mentioned above, the parameters d, f, and $1-e$ are approximately equal to 1; thus, the amplitude items contained in Eqs. (48) and (49) are not zero. Therefore, the retardations $\varphi_2(\sigma)$ and $\varphi_1(\sigma)+\varphi_2(\sigma)$ can be obtained by taking the argument of the results of Eqs. (48) and (49), respectively.

In the presented method, we use two linearly polarized beams with a relative angle of 45° to perform the calibration of a channeled spectropolarimeter. During the calibration process, we substitute the requirement of an absolute angle by a relative angle, making the calibration of the instrument easy to implement in the laboratory. Using the calibration model derived above and the measurement data of the calibration process, we can quickly solve the alignment and retardation errors that need to be calibrated in the modified reconstruction model.

B. Compensation of the Influences of Alignment and Retardation Errors

Since the alignment errors and the actual phase factors contained in the modified reconstruction model are settled, we can utilize the calibration results to compensate for the influences of alignment and retardation errors. It is a software compensation without any mechanical precision adjustment of polarization elements.

According to the modified reconstruction model, we can also utilize the desired channels C_0, C_2, and C_3 to demodulate the polarization contents of a target light. First, we eliminate the phase factors using the actual retardations calibrated above to compensate for the retardation errors of the high-order retarders. The results after compensation of the retardation errors are given by

$$\Gamma\{C_0'(h)\} = \frac{1}{2}S_0(\sigma), \tag{50}$$

$$\Gamma\{C_2'(h)\} = \frac{1}{4}df\{b \cdot S_1(\sigma) + a \cdot S_2(\sigma)\}, \tag{51}$$

$$\Gamma\{C_3'(h)\} = \frac{1}{8}d(1-e)\{a \cdot S_1(\sigma) - b \cdot S_2(\sigma) - iS_3(\sigma)\}. \tag{52}$$

Then, we utilize the calibration results of the alignment errors to demodulate the true Stokes parameters contained in different channels, given by

$$S_0(\sigma) = 2|\Gamma\{C_0'(h)\}|, \tag{53}$$

$$S_1(\sigma) = \frac{1}{a^2+b^2}\left\{4 \cdot \frac{b|\Gamma\{C_2'(h)\}|}{df} + 8 \cdot \frac{a\mathrm{Re}[\Gamma\{C_3'(h)\}]}{d(1-e)}\right\}, \tag{54}$$

$$S_2(\sigma) = \frac{1}{a^2+b^2}\left\{4 \cdot \frac{a|\Gamma\{C_2'(h)\}|}{df} - 8 \cdot \frac{b\mathrm{Re}[\Gamma\{C_3'(h)\}]}{d(1-e)}\right\}, \tag{55}$$

$$S_3(\sigma) = \mathrm{Im}\left[-8 \cdot \frac{\Gamma\{C_3'(h)\}}{d(1-e)}\right]. \tag{56}$$

Since the alignment and retardation errors of high-order retarders are considered in the presented reconstruction method, the reconstructed Stokes vector will be more accurate. Though the form of the derived calibration and compensation models looks more complex compared to the theoretical reconstruction model for the channeled spectropolarimeter, the added parts are only the simple trigonometric functions, four-arithmetic operations, and general phase unwrapping calculations, which will not lead to difficulties in the practical measurement process of a channeled spectropolarimeter.

4. VERIFICATION BY NUMERICAL SIMULATIONS

The effectiveness and feasibility of the presented method are verified by numerical simulations. In the simulations, the target light to be measured is a linearly polarized light, oriented at 30°. The wavenumber range is 14,954–18,408 cm^{-1}, and the thicknesses of R_1 and R_2 are 3 mm and 6 mm, respectively. The high-order retarders are made of quartz, and the dispersion of birefringence of quartz is considered during the simulation process. The birefringence of high-order retarders in the selected waveband can be consulted in Ref. [15].

The magnitude of the autocorrelation function of the obtained spectrum without the influences of alignment and retardation errors is shown below.

As shown in Fig. 3, owing to the thickness ratio of high-order retarders being 1:2, the seven channels included in $C(h)$ are satisfactorily separated from one another over the h axis [23]. The desired channels C_0, C_2, and C_3 are centered at $h = 0$, $h = 27.18$ μm, and $h = 81.54$ μm. It is consistent with the theoretical model calculation, which verifies the validity of the numerical simulations.

We first demonstrate the influences of alignment and retardation errors on the accuracy of the reconstructed polarization parameters by simulations. The results are shown in Fig. 4.

As shown in Fig. 4, the reconstruction accuracy of the polarization parameters decreases as the alignment and retardation errors increase. Referring to the specifications of aerosol polarimetry sensor (APS) introduced in Eq. (23), the influences of the alignment and retardation errors of high-order retarders on the accuracy of a channeled spectropolarimeter cannot be ignored. Owing to the input value of S_3/S_0 close to zero, the reconstruction accuracy of S_3/S_0 is not very sensitive to the alignment errors as are other polarization parameters. However, it is so sensitive to the retardation errors that even the input value is small, and the deviations of S_3/S_0 are more distinct

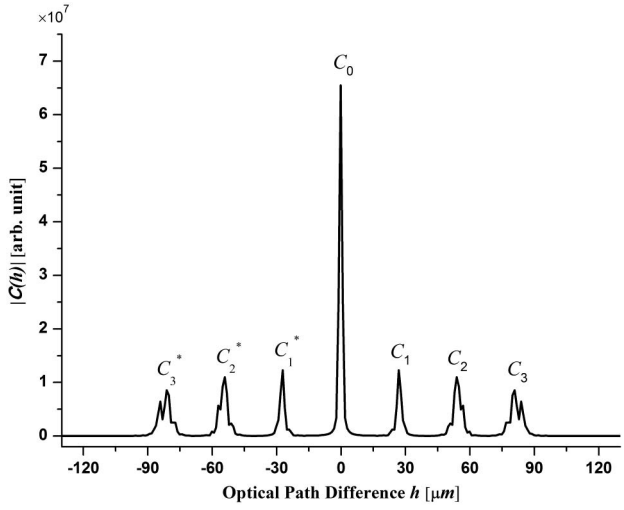

Fig. 3. Magnitude of the autocorrelation function of the modulated spectrum.

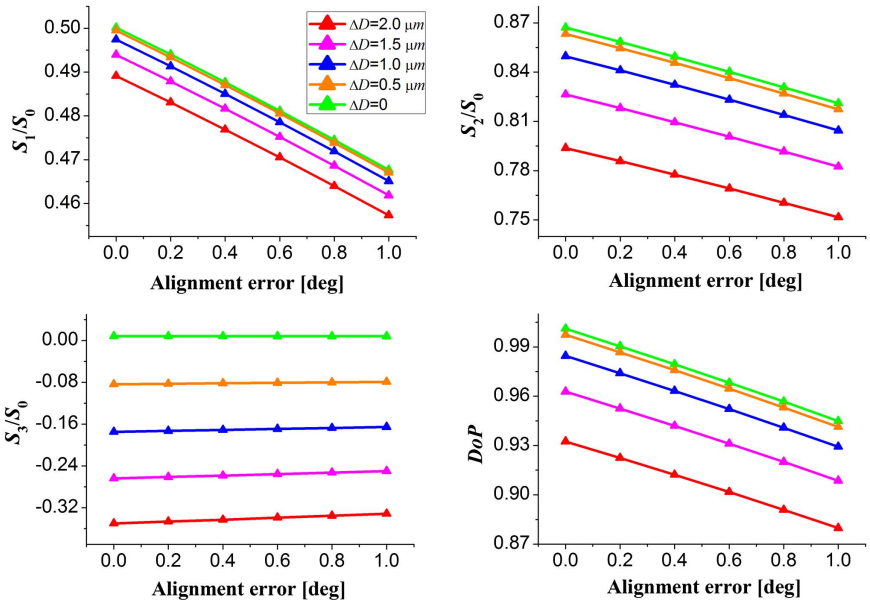

Fig. 4. Influences of alignment and retardation errors on the accuracy of the reconstructed polarization parameters at the wavenumber 18408 cm^{-1}. The input values are $S_1/S_0 = 0.5$, $S_2/S_0 = 0.866$, $S_3/S_0 = 0$, and DoP = 1.

than other polarization parameters. It also implies that to fully evaluate the precision of a polarization measurement for the channeled spectropolarimeter, the specifications of the normalized Stokes parameters should be considered during the development and practical application stages of the instrument.

Then, we simulate the reconstruction process of polarization parameters in a specific situation such that the alignment errors are $\varepsilon_1 = -\varepsilon_2 = -0.5°$ and the thickness errors are $\Delta D_1 = \Delta D_2 = 2$ μm. The effectiveness of the presented method to calibrate and compensate the alignment and retardation errors of high-order retarders is shown in Figs. 5–7 and Tables 2–4.

The calculation results of the alignment errors of high-order retarders are shown in Fig. 5 and Table 2 when the input values are $\varepsilon_1 = -\varepsilon_2 = -0.5°$. The maximum calculated errors of R_1 and R_2 are −0.056° and 0.027°, respectively. Because the alignment errors are independent of wavenumber, we can use the averages of the calculated values in different wavenumbers as the final calculation results. Therefore, the deviations of alignment errors of R_1 and R_2 are −0.012° and 0.013°, respectively. These results indicate that we can calibrate the alignment errors accurately using the presented method. This is significant for reconstructing polarization parameters.

The calibration results of retardation of high-order retarders are shown in Fig. 6 and Table 3 when the thickness errors of R_1 and R_2 are set to $\Delta D_1 = \Delta D_2 = 2$ μm. As shown in Figs. 6(c) and 6(d), the actual retardations of high-order retarders have obviously deviated from the nominal values when the thickness errors are $\Delta D_1 = \Delta D_2 = 2$ μm. The retardation errors of R_2 and $R_1 + R_2$ between the actual values and the nominal values at the selected wavenumber of $\sigma = 18408 cm^{-1}$ are 0.212 rad and 0.424 rad, respectively. Therefore, we cannot directly use the nominal values to eliminate the phase factors during the reconstruction process of the polarization parameters. In contrast, the calibration results obtained by the presented method are almost consistent with the actual values. The deviations of retardations of R_2 and $R_1 + R_2$ at the selected wavenumber of $\sigma = 18408 cm^{-1}$ are 0.002 rad and 0.010 rad, respectively. The results demonstrate that using the presented method

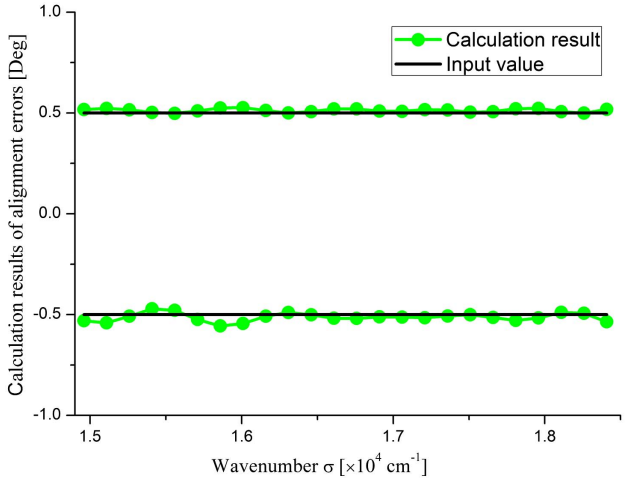

Fig. 5. Calculation results of the alignment errors of high-order retarders R_1 and R_2. The input values are $\varepsilon_1 = -0.5°$ and $\varepsilon_2 = 0.5°$.

Table 2. Calculation Results of the Alignment Errors ε_1 and ε_2

Parameter	Input Value	Calculated Value	Maximum Calculated Error	Average Calculated Error
ε_1	−0.5°	−0.512°	−0.056°	−0.012°
ε_2	0.5°	0.513°	0.027°	0.013°

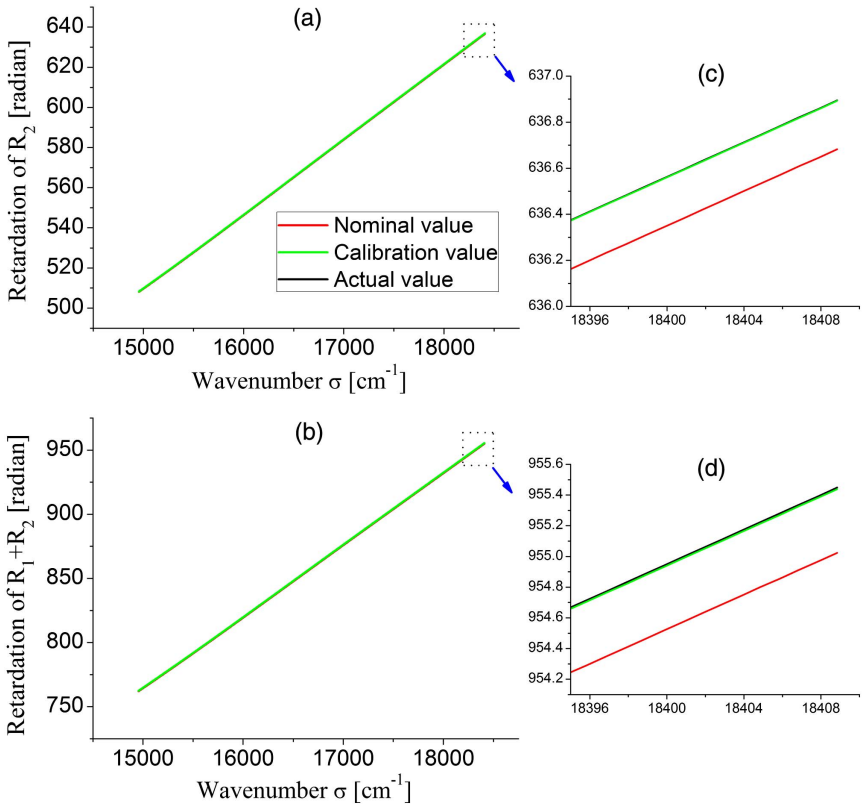

Fig. 6. Calibration results of retardations of high-order retarders R_1 and R_2. (c) and (d) are the enlarged part in the dashed box of (a) and (b), respectively.

Table 3. Comparison of Retardations of R_1 and R_2 at the Selected Wavenumber of $\sigma = 18408\ \text{cm}^{-1}$ when the Thickness Errors Are $\Delta D1 = \Delta D2 = 2\ \mu\text{m}$

Parameter	Nominal Value	Calibration Value	Actual Value
φ_2	636.64 rad	636.86 rad	636.86 rad
$\varphi_1 + \varphi_2$	954.97 rad	955.38 rad	955.39 rad

can determine the actual retardations of high-order retarders. It is important for eliminating the phase factors contained in Eqs. (28) and (29) to discover the true polarization contents of a target light.

As shown in Figs. 6(a) and 6(b), the retardation errors of high-order retarders may be not distinct enough, but their influences on the accuracy of reconstructed polarization parameters are significant. The effects of retardation errors on the reconstructed polarization parameters and the effectiveness of the presented method to keep the accuracy when the alignment and retardation errors existing are shown in Fig. 7.

As shown in Fig. 7 and Table 4, the reconstruction errors of polarization parameters are reduced by more than 1 order of magnitude by utilizing the presented calibration method to compensate for the alignment and retardation errors of high-order retarders. The above results demonstrate that the influences of the alignment and retardation errors have been mitigated greatly. This calibration method is effective for achieving high precision of the instrument while relaxing the tolerance of assembly errors of the PSIM module. Furthermore, the presented method can work effectively without any precise mechanical adjustments. The advantage of easy implementation makes this calibration method more suitable to apply in the laboratory and to be on track for correcting the channeled spectropolarimeter.

It is worthy to emphasize that during the whole simulation process, the noise effects, which have significant influences on the calibration precision of the alignment errors, are ignored. To address this problem, there are some effective ways for selecting them in practical applications. The first way is that, considering the advantage of the simplicity of the optical system (the PSIM module can be regarded as a whole component to be inserted into the optical system) [7], the PSIM module can be calibrated separately using a stable spectrometer with high signal-to-noise ratio (SNR). The second way is that we can use a suitable metric to optimize the configuration of the instrument for making it immune to noise. Mu *et al.* have proposed a metric for the optimization of broadband full-Stokes polarimeters, named the optimally balanced condition for Poisson noise (BCPN) [24]. The polarimeters optimized with the BCPN have immunity to both Poisson and Gaussian noise. Furthermore, while the polarimeter optimized from the commonly used optimization metrics, such as the condition number (CN), the equally weighted variance (EWV), and the polarimetric modulation efficiency (PME), is recognized as a polychromatic one, the polarimeter optimized from the BCPN can be achromatic. In Ref. [25], Quan *et al.* also introduce an optimal configuration to decrease the measurement variance in

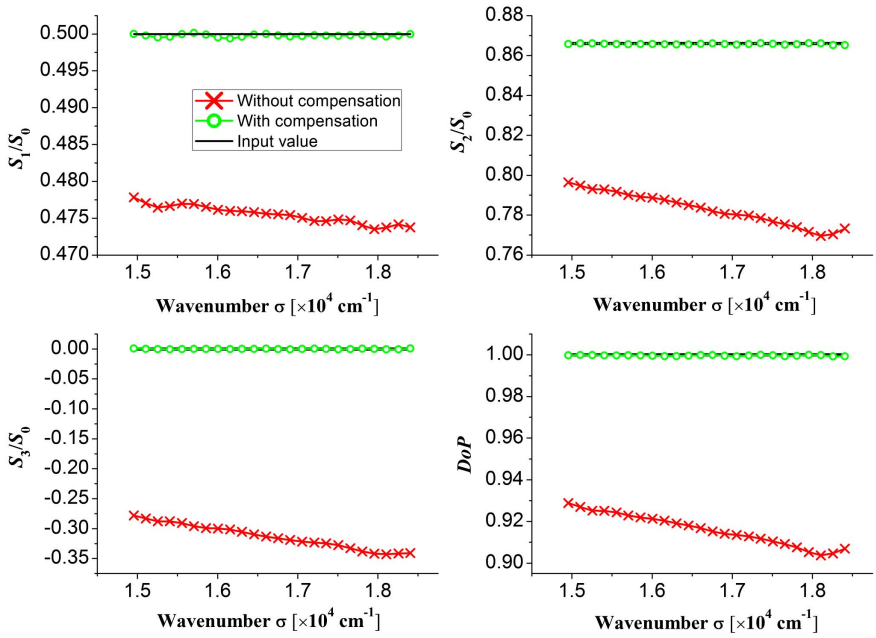

Fig. 7. Comparison of reconstructed results of polarization parameters (a) without compensation, (b) with compensation by the presented method. The input values are $S_1/S_0 = 0.5$, $S_2/S_0 = 0.866$, $S_3/S_0 = 0$, and DoP = 1.

Table 4. Comparison of Reconstructed Results of Polarization Parameters at the Selected Wavenumber of $\sigma = 18408\ \text{cm}^{-1}$

Situation	S1/S0 Error	S2/S0 Error	S3/S0 Error	DoP Error
Without compensation	-2.62×10^{-2}	-9.27×10^{-2}	-3.41×10^{-1}	-9.31×10^{-2}
With compensation	-4.41×10^{-5}	-7.85×10^{-4}	6.83×10^{-4}	-7.24×10^{-4}

the presence of additive Gaussian noise and signal-dependent shot noise [25]. The last way is that we may select some special reference beams to make the calibration process insensitive to the noise. Mu *et al.* have presented a paradigm for selecting reference polarization states to improve the precision of the estimated system matrix in the presence of noise [26]. During the experimental tests, to minimize the effects of noises, we select a stable spectrometer (FieldSpec 3, Analytical Spectral Devices) with very high SNR to record the spectrum.

5. ANALYSES OF EXPERIMENTAL RESULTS

The validity of the presented method is further verified by experimental tests. The experimental configuration can be seen in Fig. 8, where the channeled spectropolarimeter consists of the PSIM module (the retarders R_1 and R_2 and polarizer A in the dashed box) and a spectrometer (FieldSpec 3, Analytical Spectral Devices), and the high-stability broadband light source consists of a stabilized tungsten halogen lamp and a collimator. The rotatable polarizer P is used to generate the target light oriented at 30° and two linearly polarized beams whose polarization orientation crossing at 45°.

The thicknesses of R_1 and R_2 and the wavenumber range are consistent with the simulation settings. The retarders R_1 and R_2 and polarizers A and P are placed in precision-adjusting racks for assembling the experimental configuration as well as possible.

After assembling the experimental setup, we measure the modulated spectrum illuminating the system with the target light, a linearly polarized light, oriented at 30°. The magnitude of the autocorrelation function of the obtained spectrum is shown below.

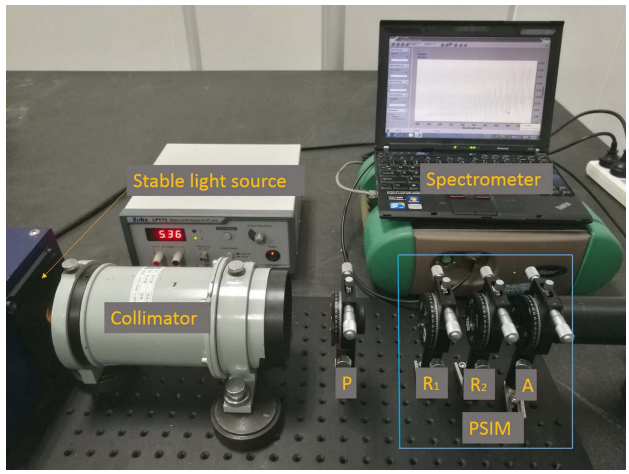

Fig. 8. Photograph of the experimental setup.

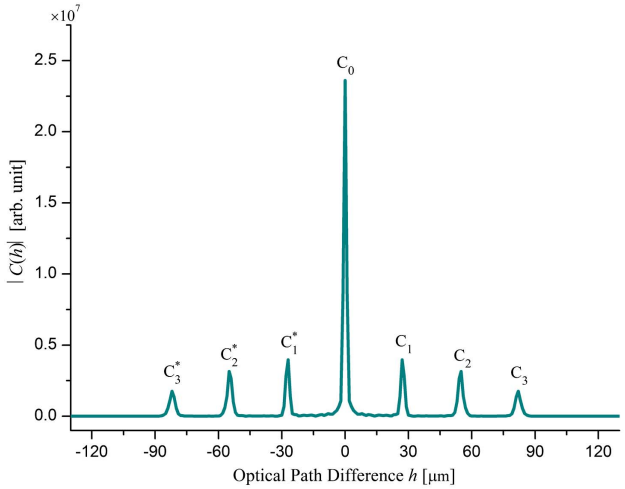

Fig. 9. Magnitude of the autocorrelation function of the modulated spectrum illuminating with a linearly polarized light, oriented at 30°.

As shown in Fig. 9, the seven channels are separated from one another over the h axis, consistent with the modified reconstruction model and simulation results. Because the influences of alignment and retardation errors on the frequency spectrogram are relative unapparent, next we demodulate the polarization parameters from the frequency spectrogram. The reconstruction results of polarization parameters ignoring the alignment and retardation errors are presented in Figs. 10(a)–10(d). As introduced in Section 1, owing to the inevitable alignment errors and the thickness errors (caused by manufacture tolerance) of two high-order retarders, the reconstructed polarization parameters obviously fluctuate from their input values. As a contrast, the reconstruction results of polarization parameters after calibration and compensation with the presented method are presented in Figs. 10(e)–10(h).

As shown in Figs. 10(a)–10(d), the reconstructed results ignoring the alignment and retardation errors have deviated from the input values severely, indicating that the alignment and retardation errors of high-order retarders will decrease the accuracy of a channeled spectropolarimeter. By employing the presented method to calibrate and compensate the alignment and retardation errors, the precision of the channeled spectropolarimeter has been improved greatly. The comparison of reconstructed results is shown in Table 5, demonstrating the effectiveness of the presented method in reducing the influences of the alignment and retardation errors of high-order retarders.

There are two things to explain. First, the reconstructed results of the polarization parameters after compensation are not consistent with the input values; specifically, the average value of S_1/S_0 is less than 0.5 and the average value of S_2/S_0 is more than 0.866, possibly because the orientation of the target light is bigger than 30°. Second, the fluctuation of experimental results is larger than the simulations, and the accuracy of experimental tests is lower than the simulations. This may be affected by the vibration of reconstructed results; although, we have alleviated the influences by introducing apodization using the Hann window [16] and the environmental factors, such as noise and stray light [12]. Overall, the presented method is

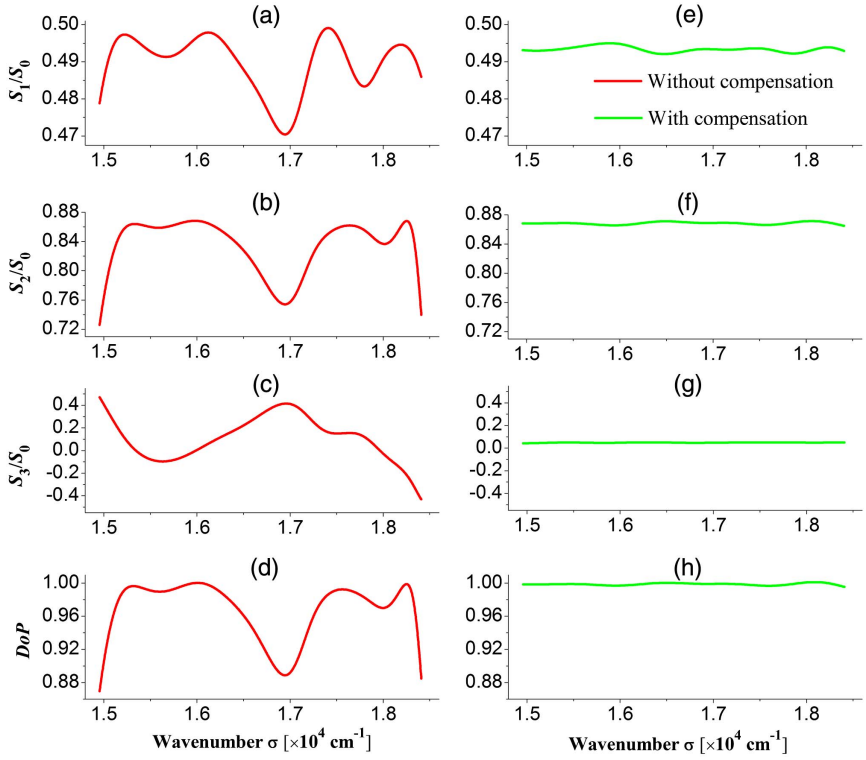

Fig. 10. Comparison of reconstructed results (a)–(d) without compensation, (e)–(h) with compensation by the presented method. The input values are $S_1/S_0 = 0.5$, $S_2/S_0 = 0.866$, $S_3/S_0 = 0$, and DoP = 1.

Table 5. Comparison of Reconstructed Polarization Parameters without/with Compensation by the Presented Method

Situation	Deviation Type	S1/S0 Error	S2/S0 Error	S3/S0 Error	DoP Error
Without compensation	Maximum	-2.96×10^{-2}	-1.40×10^{-1}	4.73×10^{-1}	1.31×10^{-1}
	Average	-1.02×10^{-2}	-3.06×10^{-2}	1.10×10^{-1}	3.15×10^{-2}
With compensation	Maximum	-7.93×10^{-3}	5.38×10^{-3}	5.15×10^{-2}	-4.63×10^{-3}
	Average	-6.62×10^{-3}	2.37×10^{-3}	4.85×10^{-2}	-1.25×10^{-3}

effective in calibrating and compensating for the alignment and retardation errors to improve the accuracy of a channeled spectropolarimeter. It is significant for the quantitative application of the channeled spectropolarimeter.

6. CONCLUSIONS

The alignment and retardation errors of high-order retarders will decrease the accuracy of the channeled spectropolarimeter apparently. In this paper, we first theoretically derive the calibration and compensation model of the alignment and retardation errors based on the modified reconstruction model considering the alignment errors. Then, we put forward a calibration method to reduce the influences of alignment and retardation errors of high-order retarders for keeping the accuracy of the channeled spectropolarimeter. The presented method is easier to implement than the other methods. The reason is that the presented method requires only rotating a relative angle based on the auxiliary polarizer's coordinate system while other methods require making sure that this coordinate system and the global coordinate system of the instrument cross at an absolute angle. Simulation results show that by utilizing the presented method, the maximum and average reconstruction errors of the polarization parameters are reduced by at least 1 order of magnitude. The effectiveness of the presented method is further verified by experiments. By employing the presented method, we can relax the alignment tolerances of the PSIM module elements in the ground-based assembly of the channeled spectropolarimeter. Furthermore, even when the instrument works in orbit, using this method for regular correction is still effective and convenient to maintain the accuracy and stability of polarization measurement for the channeled spectropolarimeter. It has an important significance for the quantitative application of the channeled spectropolarimeter.

Funding. National Natural Science Foundation of China (NSFC) (61505199); National Key Research and Development Program (2016YFF0103603).

REFERENCES

1. D. J. Diner, R. A. Chipman, N. Beaudry, B. Cairns, L. D. Food, S. A. Macenka, T. J. Cunningham, S. Seshadri, and C. Keller, "An integrated multiangle, multispectral, and polarimetric imaging concept for aerosol remote sensing from space," Proc. SPIE **5659**, 88–96 (2005).
2. S. H. Jones, F. J. Iannarilli, C. Hostetler, B. Cairns, A. Cook, J. Hair, D. Harper, Y. Hu, and D. Flittner, "Preliminary airborne measurement results from the hyperspectral polarimeter for aerosol retrievals (HySPAR)," in *NASA Earth Science Technology Conference Proceedings* (2006), pp. 1–6.
3. N. Gupta and D. R. Suhre, "Acousto-optic tunable filter imaging spectrometer with full Stokes polarimetric capability," Appl. Opt. **46**, 2632–2637 (2007).
4. N. Gupta, "Acousto-optic tunable filter based spectropolarimetric imagers," Proc. SPIE **6972**, 69720C (2008).
5. B. P. Cumming, G. E. Schröder-Turk, S. Debbarma, and M. Gu, "Bragg-mirror-like circular dichroism in bio-inspired quadruple-gyroid 4srs nanostructures," Light Sci. Appl. **6**, e16192 (2017).
6. A. Y. Zhu, W. T. Chen, A. Zaidi, Y. Huang, M. Khorasaninejad, V. Sanjeev, C. Qiu, and F. Capasso, "Giant intrinsic chiro-optical activity in planar dielectric nanostructures," Light Sci. Appl. **7**, 17158 (2018).
7. K. Oka and T. Kato, "Spectroscopic polarimetry with a channeled spectrum," Opt. Lett. **24**, 1475–1477 (1999).
8. F. J. Iannarilli, S. H. Jones, H. E. Scott, and P. L. Kebabian, "Polarimetric-spectral intensity modulation (P-SIM): enabling simultaneous hyperspectral and polarimetric imaging," Proc. SPIE **3698**, 474–481 (1999).
9. A. Taniguchi, H. Okabe, H. Naito, N. Nakatsuka, and K. Oka, "Stabilized channeled spectropolarimeter using integrated calcite prisms," Proc. SPIE **5888**, 588811 (2005).
10. A. Taniguchi, K. Oka, H. Okabe, and M. Hayakawa, "Stabilization of a channeled spectropolarimeter by self-calibration," Opt. Lett. **31**, 3279–3281 (2006).
11. T. Mu, C. Zhang, C. Jia, W. Ren, L. Zhang, and Q. Li, "Alignment and retardance errors, and compensation of a channeled spectropolarimeter," Opt. Commun. **294**, 88–95 (2013).
12. B. Yang, X. Ju, C. Yan, and J. Zhang, "Alignment errors calibration for a channeled spectropolarimeter," Opt. Express **24**, 28923–28935 (2016).
13. X. Ju, B. Yang, J. Zhang, and C. Yan, "Reduction of the effects of angle errors for a channeled spectropolarimeter," Appl. Opt. **56**, 9156–9164 (2017).
14. J. Li, J. Zhu, and H. Wu, "Compact static Fourier transform imaging spectropolarimeter based on channeled polarimetry," Opt. Lett. **35**, 3784–3786 (2010).
15. G. Ghosh, "Dispersion-equation coefficients for the refractive index and birefringence of calcite and quartz crystals," Opt. Commun. **163**, 95–102 (1999).
16. D. S. Sabathe, "Snapshot spectropolarimetry," Ph.D. dissertation (University of Arizona, 2002).
17. D. J. Diner, R. A. Chipman, N. Beaudry, B. Cairns, L. D. Foo, S. A. Macenka, and C. Keller, "Enabling sensor and platform technologies for spaceborne remote sensing," Proc. SPIE **5659**, 88–96 (2005).
18. R. J. Peralta, C. Nardell, B. Cairns, E. E. Russell, L. D. Travis, M. I. Mishchenko, and R. J. Hooker, "Aerosol polarimetry sensor for the Glory Mission," Proc. SPIE **6786**, 67865L (2007).
19. S. Persh, Y. J. Shaham, O. Benami, B. Cairns, M. I. Mishchenko, J. D. Hein, and B. A. Fafaul, "Ground performance measurements of the Glory aerosol polarimetry sensor," Proc. SPIE **7807**, 780703 (2010).
20. C. Zhang, N. Quan, and T. Mu, "Stokes imaging spectropolarimeter based on channeled polarimetry with full-resolution spectra and aliasing reduction," Appl. Opt. **57**, 6128–6134 (2018).
21. N. Quan, C. Zhang, T. Mu, and Q. Li, "Channeled polarimetric technique for the measurement of spectral dependence of linearly Stokes parameters," Infrared Phys. Technol. **90**, 95–100 (2018).
22. N. Quan, C. Zhang, and T. Mu, "Full linearly Stokes channeled polarimetric technique with low reconstruction errors," Optik **164**, 36–44 (2018).
23. N. Hagen, A. M. Locke, D. S. Sabatke, E. L. Dereniak, and D. T. Sass, "Methods and applications of snapshot spectropolarimetry," Proc. SPIE **5432**, 167–174 (2004).

24. T. Mu, Z. Chen, C. Zhang, and R. Liang, "Optimal design and performance metric of broadband full-Stokes polarimeters with immunity to Poisson and Gaussian noise," Opt. Express **24**, 29691–29704 (2016).
25. N. Quan, C. Zhang, and T. Mu, "Optimal configuration of partial Mueller matrix polarimeter for measuring the ellipsometric parameters in the presence of Poisson shot noise and Gaussian noise," Photon. Nanostr. Fundam. Appl. **29**, 30–35 (2018).
26. T. Mu, D. Bao, C. Zhang, Z. Chen, and J. Song, "Optimal reference polarization states for the calibration of general Stokes polarimeters in the presence of noise," Opt. Commun. **418**, 120–128 (2018).